

Reversible wettability of optothermal responsively perfluoroalkyl azobenzene self-assembled monolayers

Li Dai^{a,b}, Lu Cai^{a,b}, Yanhua Yuan^{a,b}, Anqi Liu^{a,b}, Zhanxiong Li^{a,b,*}

^aCollege of Textile and Clothing Engineering, Soochow University, Suzhou 215021, China

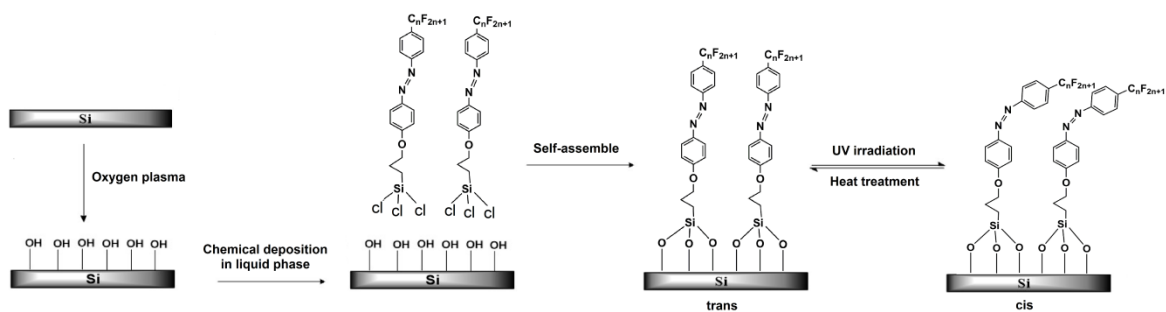
^bNational Engineering Laboratory for Modern Silk, Suzhou 215123, China

*Corresponding author at: College of Textile and Clothing Engineering, Soochow University, No. 199 Renai Road, Industry Park, Suzhou 215021, China Tel: +86-512-67061190; Fax: +86-512-67246786. E-mail address: lizhanxiong@suda.edu.cn (Z. X. Li).

Abstract

In this study, two perfluoroalkyl azobenzene trichlorosilanes were synthesized and then characterized by Fourier Transform Infrared Spectroscopy (FT-IR), ¹H NMR and ¹⁹F NMR. Subsequently, these fluorine containing trichlorosilanes were applied to form self-assembled monolayers (SAMs) on silicon substrates by the method of chemical deposition in liquid phase. The optothermal responsively isomerization of the azobenzene was achieved *via* UV irradiation and heat treatment. The surface structures of the SAMs were investigated by X-ray photoelectron spectroscopy (XPS), energy dispersive X-ray spectroscopy (EDS) and atomic force microscopy (AFM). The results showed that the thermal migration of the terminal fluoroalkyl groups promoted the isomerization of the azo-groups. Moreover, the reversible contact angles of the SAMs demonstrated a good reversibility of surface wettability, which was consistent with the

optothermal responsive isomerization of the azo-groups.



Keywords

Self-assembled monolayers; optothermal response; perfluoroalkyl azobenzene; reversible isomerization

Introduction

In the past decades “smart surfaces” have attracted more and more attention due to their controlled switchable functions in respond to even slight changes in stimuli of the surroundings, which can be temperature, pH, light, magnetic or electric field etc.¹⁻³ Meanwhile these surfaces have many potential applications in various fields, such as biosensors, microfluidic devices and intelligent membranes.⁴⁻⁶ Photoresponsive smart surfaces have attracted great interest in recent years and have been applied in non-linear optics, microelectronics, photoresponsive materials and optical data storage.⁷⁻⁹ According to previous studies of photoresponsive surfaces, azobenzene and its derivatives are well known to show great changes in molecular configuration as a result of photoisomerization.¹⁰ As photoactive chemicals, they can experience transition from the *trans* isomer (which is stable under the environment conditions) to the *cis* isomer by UV irradiation.^{7,11-15} Moreover, the back *cis-to-trans* conversion can be achieved by two important ways: (i) irradiation by visible light with wavelength in the range of 400 - 500 nm and (ii) keeping in a dark place or thermal back relaxation.¹⁶⁻¹⁷

During the *cis-to-trans* isomerization of azobenzene the wettability of the azobenzene modified surfaces changed as the *trans* isomer with a small dipole moment has a low surface free energy, while the *cis* isomer with a larger dipole moment has a higher surface free energy.¹⁸⁻¹⁹ Although the wettability of azobenzene has been extensively studied, most azobenzene modified

surfaces prepared on flat substrates exhibited only a minor change in CA, which was about 10° ,¹⁸⁻²³ except studies, which were reported in recent years combining with some other properties or technologies, such as the roughness of substrates, nanotechnology and electrostatic technology, etc.²⁴⁻²⁷ The good reversible wettability of azobenzene and its derivative had been studied by many researchers.^{28,29}

Due to the unique properties of C-F bonds including excellent chemical and thermal stability, low refractive index, predominant hydrophobicity and oleophobicity,^{30,31} perfluorinated compounds have been widely applied in a variety of fields.^{32,33} These fluorine containing materials possess low surface energy, because fluorine with its high electronegativity can reduce the internal van der Waals interactions. Even monolayers of perfluorinated compounds can provide extreme low surface energy. In the monolayer, the fluoroalkyl groups can migrate from the inner part of the films to the outermost surface, which is the so called “microphase separation”.³⁴

In this study, perfluoroalkyl groups have been introduced to azobenzene and prepared to form SAMs on silicon substrates.³⁵⁻³⁷ The optothermal response of perfluoroalkyl azobenzene SAMs was studied by UV irradiation and heat treatment and the surface properties were characterized by Fourier transform infrared spectroscopy, UV-visible absorption spectra, contact angle measurement, energy dispersive X-ray spectroscopy and atomic force microscopy.

Results and discussion

UV-visible absorption spectra of PFBTPA

The UV-visible absorption spectra of PFBTPA were recorded in toluene solution before and after the solution of PFBTPA was irradiated by UV light for different time periods in the range of 0 - 8 min, using a long wave-length UV lamp and are shown in Figure 1. Two absorption peaks were observed for each irradiation time period. One peak was at 360 nm, which can be assigned to the π - π^* band of the *trans* isomer, showing an obvious decrease tendency with the increase of irradiation time. The other weaker peak was observed at 450 nm and can assigned to the π - π^* band of the *cis* isomer, showing a clear increase tendency with the increase of irradiation time. As was reported,^{2,43-46} there was an observable change in the height of the *trans* isomer peak after irradiation by UV light. In addition, when the solution which had been irradiated by UV light, was warmed up to high temperatures, the UV-visible absorption spectra showed a reversion (Figure 2), which demonstrated that optothermal isomerization of the azobenzene occurred (Figure 3).

X-Ray photoelectron spectroscopy

The surface chemical composition of the SAMs was investigated by X-ray photoelectron spectroscopy (XPS). The wide scans spectra of PFBTPA SAMs before and after heat treatment were measured and are shown in Figure 4. Table 1 lists the chemical composition of PFBTPA SAMs before and after heat treatment. The mass concentration of fluorine on the surface of PFBTPA SAMs was 31.24 % after heat treatments, which is higher than the value of 28.26 %

before heat treatment. The apparent increase of fluoroalkyl groups content on the surface of the SAMs can be ascribed to the isomerization of the azobenzene during the heat treatment.

Water contact angles

The wettability can be affected by the chemical composition and roughness of the substrates.¹⁰

The water contact angle is quite sensitive to a change in surface properties and it has been widely used for the investigation of the isomerization of azo groups on surfaces.

Figure 5 shows the contact angles of different SAMs. As shown, it can be found that the contact angles of PFHTPA SAMs were higher than those of PFBTPA SAMs because the former possesses a longer terminated fluorocarbon chain bonded to the azobenzene. As is shown, the water contact angles of PFBTPA SAMs and PFHTPA SAMs before heat treatment were $88.7 \pm 1.0^\circ$ and $96.1 \pm 1.2^\circ$, while those of PFBTPA SAMs and PFHTPA SAMs after heat treatment were $102.1 \pm 1.4^\circ$ and $111.4 \pm 0.6^\circ$ respectively, implying a more hydrophobic surface after heat treatment. This may be attributed to the inherent migration of fluoroalkyl chains under high temperature and it indicates that the *cis* configuration of the azo groups has changed into a *trans* configuration during the heat treatment.⁴⁷

On the contrary, the water contact angles of PFBTPA SAMs and PFHTPA SAMs decreased to $83.3 \pm 2.4^\circ$ and $89.1 \pm 1.5^\circ$, respectively, after UV light irradiation. This result showed, that the differences between SAMs-heat and SAMs-UV were nearly 20° , which was much larger than the results reported in previous studies.¹⁸⁻²³ This was due to the fact that thermal migration of

terminal fluoroalkyl groups can promote the isomerization of the azobenzene and further decrease the surface free energy simultaneously.

Figure 6 shows the contact angles of SAMs under repeated UV irradiation and then heat treatment. The results clearly show, that the contact angles of SAMs irradiated by UV light almost completely recovered after heating treatment and decreased again when irradiated by UV light. As a result, a surface with good reversible wettability was observed.

Energy dispersive X-ray spectroscopy

The distribution of elements on the surface of PFBTPA SAMs was characterized by energy dispersive X-ray spectroscopy (EDS) and the results are shown in Figures 7a-d. As can be seen, C, O, Si and F were detected on PFBTPA SAMs surface. Figure 7e shows the distribution of F on the surface of heated PFBTPA SAM, which has been treated at 160 °C for 1 h before the measurement. Comparing Figures 7d and 7e, an obvious increase of the fluorine content on the surface of PFBTPA SAMs after heat treatment was found because of the migration of fluoroalkyl groups and *cis* to *trans* isomerization of azobenzene. However, the distribution of F on the SAM surface decreased after irradiation by UV light, implying that photoisomerization of azobenzene from *trans* to *cis* configuration occurred.

Surface morphology and surface roughness

The surface morphologies of the pure silicon substrate and PFBTPA SAMs on silicon were obtained by AFM. Compared with the flat surface of pure silicon substrate (Figures 8a and 8c),

many highlight dots were found on the surface of PFBTPA SAM (Figure 8c). The AFM results demonstrated that some sharp peaks have been formed on the SAM (Figure 8d). These sharp peaks resulted in an increase of surface roughness, which made the surface become more sensitive to the slight change of surface tension. Thus, the slight change of configuration can lead to a measurable change of surface wettability.

Table 2 shows the surface roughness of the bare silicon substrate and PFBTPA SAMs. R_a and R_q of silicon substrate surface before and after self-assemble were calculated by equations (1) and (2). The result showed that the values of R_a and R_q increased to 0.591 nm and 0.826 nm after PFBTPA self-assemble.

$$R_a = \frac{1}{l} \int_0^l |z(x)| dx \quad (1)$$

$$R_q = \sqrt{\frac{1}{l} \int_0^l z^2(x) dx} \quad (2)$$

R_a is the arithmetical mean deviation of assessed profile, l is sampling length, and $z(x)$ is the height of the assessed profile at any position x . R_q is the mean square deviation of the assessed profile.⁴⁸

Conclusions

In summary, fluoroalkyl trichlorosilanes with different perfluoroalkyl carbon chain length bonded to azobenzene were synthesized and characterized by FT-IR, ^1H NMR and ^{19}F NMR. UV-visible absorption spectra showed a transition of *trans* to *cis* configuration of the fluoroalkyl trichlorosilanes when irradiated by UV light and a transition of *cis* to *trans* configuration of the

fluoroalkyl trichlorosilanes after heat treatment. Afterwards, self-assembled monolayers of PFBTPA and PFHTPA on silicon wafers were successfully prepared through the method of liquid phase deposition. Water contact angles of PFBTPA SAMs demonstrated a good reversibility of surface wettability, which was consistent with the optothermal responsive isomerization of the azo-groups. Meanwhile, because the thermal migration of terminal fluoroalkyl groups can promote the isomerization process, the observed change of contact angle was up to 20° before and after isomerization. Energy dispersive X-ray spectroscopy (EDS) revealed the distribution of the elements of the SAMs, which confirmed the thermal migration of the fluoroalkyl groups and the isomerization of the azobenzene.

Experimental

Materials

4-Bromoanilines (purity ≥ 99.5 %) was supplied by Shanghai Macklin Biochemical Co., Ltd. Copper powder (max, 106 μm , -140 mesh, purity ≥ 99.0 %) was obtained from ThermoFisher Scientific Co., Ltd. Perfluorobutyl iodide ($\text{C}_4\text{F}_9\text{I}$), perfluorohexyl iodide ($\text{C}_6\text{F}_{13}\text{I}$), trichlorosilane (purity ≥ 98 %), allyl bromide (purity ≥ 98 %), phenol (purity ≥ 99.0 %) and sodium nitrite (NaNO_2 , purity ≥ 99.0 %) were purchased from Shanghai J&K Scientific Ltd. Karstedt catalyst was supplied by Sinopharm Chemical Co., Ltd. One-side polished silicon wafers were purchased from Xinxing Braim Technology Co., Ltd. Hydrochloric acid (HCl , purity 36.0 % - 38.0 %), sodium hydroxide (NaOH , purity ≥ 96.0 %), dimethyl sulfoxide (DMSO , purity ≥ 99.0 %),

tetrahydrofuran (THF, purity $\geq 99.0\%$) and anhydrous diethyl ether (Et_2O , purity $\geq 99.5\%$) were obtained from Qiangsheng Functional Chemicals Co., Ltd. and used without any further purification. Toluene (purity $\geq 99.5\%$) was purchased from Qiangsheng Functional Chemicals Co., Ltd. and purified by distillation (in order to remove water from it). The Supplemental Materials contains sample ^1H and ^{19}F NMR spectra of products 2 and 3 (Figures S 1 – S 8)

Measurements

Fourier transform infrared spectroscopy (FT-IR) spectra were measured using KBr pellets with a NICOLET 5700 spectrometer. ^1H NMR spectra were recorded with an INOVA 400 MHz NMR spectrometer in deuterated chloroform (CDCl_3) with TMS as internal standard. ^{19}F NMR spectra were obtained with a Bruker DPX 300 spectrometer in deuterated chloroform (CDCl_3) with CFCl_3 as an internal reference. UV-visible absorption spectra were obtained with an UV-1800 UV spectrophotometer (Shimadzu, Japan). The water contact angle (CA) θ ($^\circ$) was measured with an OCA40 Micro at room temperature and ambient humidity. The volume of water droplet was 3 μL . Three separated substrates for each condition were measured repeatedly and each substrate was measured five separated times to avoid random error.

X-ray photoelectron spectroscopy (XPS) analysis was carried out with a Kratos Axis Ultra HAS photoelectron spectrometer (Shimadzu, Japan), which was equipped with a monochromatic Al $\text{K}\alpha$ X-ray source. The element distribution on the surface of SAMs was measured by energy dispersive X-ray spectroscopy (EDS), which was attached to a TM3030 table scanning electron

microscope. The surface morphology of SAMs was measured with Atomic Force Microscope (AFM) in standard tapping mode at room temperature.

Syntheses and characterization

The procedure for the synthesis of the perfluoroalkyl azobenzene trichlorosilanes is shown in Scheme 1. Using 4-bromoanilines and perfluoroalkyl iodide as raw materials, 4-perfluoroalkyl-4'-aminobenzene was obtained by means of single electron transfer reaction using copper powder as catalyst. Subsequently, 4-perfluoroalkyl-4'-aminobenzene and phenol were coupled to give 4-perfluorobutyl-4'-hydroxyazobenzene at 0 - 10 °C. Then, allyl bromide was sequentially added, and 4-perfluorobutyl-4'-allyloxyazobenzene was obtained with sodium hydroxide as acid-binding agent. Finally, the trichlorosilane reacted with the terminal alkylidene group of 4-perfluorobutyl-4'-allyloxyazobenzene in a hydrosilylation reaction under vacuum conditions and the final product, the perfluoroalkyl azobenzene trichlorosilane was obtained.

Synthesis of 4-perfluorobutyl-4'-aminobenzene (1a)

To a 250 mL three-necked round bottle, 4-bromoaniline (3.44 g, 20 mmol), copper powder (5 g) and 100 mL of dimethyl sulfoxide (DMSO) were added together at room temperature. The mixture was stirred and heated to 60 °C, and then perfluorobutyl iodide (C₄F₉I, 9 g, 25 mmol) dissolved in 20 mL DMSO, was added dropwise. After the addition was complete the reaction was continued for 24 h at 120 °C. After cooling to room temperature, 100 mL of water, 200 mL of diethyl ether and the crude product were added into a 500 mL beaker and the mixture was

filtered to remove the copper. The filtrate was added into a 500 mL separating funnel and the diethyl ether phase was extracted and washed 3 times with 30 mL water. Finally, the diethyl ether phase was dried over magnesium sulfate (MgSO_4) and the pure product was obtained after evaporating the solvent under reduce pressure. Dark brown liquid, yield 3.39 g (54.5 %).³⁸ FT-IR: 3405.42, 3046.5, 1522.0, 1351.0, 1235.9, 1204.7, 1132.6, 1086.4 cm^{-1} . ^1H NMR (400 MHz, CDCl_3): δ = 7.41 (d, J = 8.7 Hz, 1H), 6.71 (d, J = 8.5 Hz, 1H), 4.16 (d, J = 7.0 Hz, 1H) (Figure S1), ^{19}F NMR (376 MHz, CDCl_3): δ = -80.93 – -81.20 (m, 3F, CF_3), -109.71 (td, J = 13.3, 2.6 Hz, 2F, CF_3CF_2), -122.84 – -123.07 (m, 2F, $\text{CF}_3\text{CF}_2\text{CF}_2$), -125.54 – -125.74 (m, 2F, $\text{CF}_3(\text{CF}_2)_2\text{CF}_2$) (Figure S2).

Synthesis of 4-perfluorohexyl-4'-aminobenzene (1b)

The synthetic procedure was the same as that used for the synthesis of 4-perfluorobutyl-4'-aminobenzene (**1a**). Dark brown liquid, yield 4.32 g (52.6 %). FT-IR: 3405.2, 3051.0, 1523.6, 1362.2, 1291.0, 1240.1, 1200.4, 1145.0, 1088.1 cm^{-1} . ^1H NMR (400 MHz, CDCl_3): δ = 7.38 (d, J = 8.4 Hz, 1H), 6.75 (d, J = 8.4 Hz, 1H), 3.75 (s, 1H) (Figure S3), ^{19}F NMR (376 MHz, CDCl_3): δ = -80.97 – -81.26 (m, 3F, CF_3), -116.08 – -116.52 (m, 2F, CF_3CF_2), -122.17 (d, J = 11.4 Hz, 2F, $\text{CF}_3\text{CF}_2\text{CF}_2$), -123.11 (d, J = 2.9 Hz, m, 2F, $\text{CF}_3(\text{CF}_2)_2\text{CF}_2$), -123.40 – -123.89 (m, 2F, $\text{CF}_3(\text{CF}_2)_3\text{CF}_2$), -126.22 – -126.58 (m, 2F, $\text{CF}_3(\text{CF}_2)_4\text{CF}_2$) (Figure S4).

Synthesis of 4-perfluorobutyl-4'-hydroxyazobenzene (2a)

To a 100 mL three-necked round bottle, 4-perfluorobutyl-4'-aminobenzene (0.93 g, 3 mmol) and

2 M aqueous hydrochloric acid (10 mL) were added. The mixture was stirred and heated to dissolve 4-perfluorobutyl-4'-hydroxyazobenzene. Subsequently the mixture was cooled to 10 °C and sodium nitrite (0.45 g, 4.5 mmol) dissolved in water (10 mL) was added dropwise. After stirring for 2 h at 10 °C the mixture turned yellow. A solution of phenol (0.42 g, 4.5 mmol) in 20 mL of 1 M aqueous sodium hydroxide was then added dropwise to the mixture and the temperature was kept below 10 °C. The pH of the reaction mixture was adjusted to 6-7 with sodium bicarbonate. Finally, the crude product was obtained by filtration and was recrystallized from methanol/water (1:1) to yield the pure product. Orange red powder, yield 0.74 g (59.3 %).^{38,39} FT-IR: 3419.5, 1595.2, 1354.6, 1231.7, 1198.8, 1136.8, 1096.5 cm⁻¹. ¹H NMR (400 MHz, CDCl₃): δ = 7.96 (dd, *J* = 19.1, 8.6 Hz, 4H, *m*-protons from -OH, *m*-protons from -C₄F₉), 7.74 (d, *J* = 8.4 Hz, 2H, *o*-protons from -C₄F₉), 6.99 (d, *J* = 8.7 Hz, 2H, *o*-protons from -OH), 5.32 (s, 1H, -OH) (Figure S5).

Synthesis of 4-perfluorohexyl-4'-hydroxyazobenzene (2b)

The synthetic procedure was the same as that used for the synthesis of 4-perfluorobutyl-4'-hydroxyazobenzene (**2a**). Dark brown liquid, yield 0.81 g (52.3 %). FT-IR: 3448.0, 1596.6, 1391.68, 1248.1, 1205.0, 1143.8, 1104.7, 1010.0 cm⁻¹. ¹H NMR (400 MHz, CDCl₃): δ = 7.88 (s, 2H, *m*-protons of -C₆F₁₃), 7.76 (s, 2H, *m*-protons of -OH), 7.64 (d, *J* = 7.3 Hz, 2H, *o*-protons of -C₆F₁₃), 6.97 (s, 2H, *o*-protons of -OH), 5.36 (s, 1H, -OH) (Figure S6).

Synthesis of 4-perfluorobutyl-4'-allyloxyazobenzene (3a)

To a 100 mL three-necked round bottle, 4-perfluorobutyl-4'-hydroxyazobenzene (1.66 g, 4 mmol) dissolved in of tetrahydrofuran (THF, 30 mL) and sodium hydroxide (0.32 g, 8 mmol) dissolved in H₂O (10 mL) were added at room temperature. The mixture was stirred for 10 minutes and heated to 45 °C, then 3-bromopropene (1.07 g, 6 mmol) dissolved in of THF (20 mL) was added into the mixture dropwise for 1 h. After the addition was complete, the reaction was continued for 24 h at 45 °C. After cooling to room temperature, diethyl ether (80 mL) and the product were added into a 250 mL separating funnel; the diethyl ether phase was extracted and washed 3 times with of water (3x30 mL), then the diethyl ether phase was dried over magnesium sulfate (MgSO₄) and the crude product was obtained after evaporating the solvent under reduced pressure. Finally, the pure product was isolated by column chromatography using petrol ether as eluent. Orange red solid, yield 1.70 g (93.2 %). FT-IR: 3124.58, 2928.49, 1689.85, 1352.53, 1235.02, 1204.06, 1136.27, 1089.16 cm⁻¹. ¹H NMR (400 MHz, CDCl₃): δ = 8.00 – 7.87 (m, 4H, *m*-protons from –OH, *m*-protons from –C₄F₉), 7.73 (t, *J* = 10.5 Hz, 2H, *o*-protons from –C₄F₉), 7.04 (d, *J* = 7.8 Hz, 2H, *o*-protons from –OH), 6.08 (dq, *J* = 9.7, 5.3 Hz, 1H, CH₂=CH), 5.43 (t, *J* = 15.2 Hz, 1H, CH=CH), 5.33 (d, *J* = 10.5 Hz, 1H, CH=CH), 4.62 (dt, *J* = 28.6, 14.3 Hz, 2H, CH₂=CH) (Figure S7).

Synthesis of 4-perfluorohexyl-4'-allyloxyazobenzene (3b)

The synthetic procedure was the same as that used for the synthesis of 4-perfluorobutyl-4'-allyloxyazobenzene (**3a**). Orange red solid, yield 2.03 g (91.3 %). FT-IR:

2962.6, 1602.9, 1581.9, 1419.5, 1311.0, 1261.5, 1195.0, 1145.0, 1089.1, 1019.1. ^1H NMR (400 MHz, CDCl_3): δ = 7.90 (d, J = 8.8 Hz, 2H, *m*-protons from $-\text{C}_6\text{F}_{13}$), 7.73 (t, J = 10.3 Hz, 2H, *m*-protons from $-\text{OH}$), 7.61 (d, J = 8.5 Hz, 2H, *o*-protons from $-\text{C}_6\text{F}_{13}$), 7.07 – 6.97 (m, 2H, *o*-protons from $-\text{OH}$), 6.06 (ddd, J = 16.0, 10.7, 5.2 Hz, 1H, $\text{CH}_2=\underline{\text{C}}\text{H}$), 5.44 (d, J = 17.2 Hz, 1H, $\underline{\text{C}}\text{H}\text{H}=\text{CH}$), 5.32 (d, J = 10.5 Hz, 1H, $\text{C}\underline{\text{H}}\text{H}=\text{CH}$), 4.62 (d, J = 5.2 Hz, 2H, $\underline{\text{C}}\text{H}_2=\text{CH}$) (Figure S8).

Synthesis of 4-perfluorobutyl-4'-(trichlorosilane)propoxyazobenzene (4a, PFBTPA)

To a 50 mL three-necked round bottle, 4-perfluorobutyl-4'-allyloxyazobenzene (0.23 g, 0.5 mmol), 0.05 mL of 2 % Pt (dvs) and 20 mL toluene purified by distillation were added together under N_2 atmosphere. The mixture was stirred and heated to 70 °C, then trichlorosilane (0.15 g, 1 mmol) dissolved in 10 mL of toluene purified by distillation was added dropwise and the temperature was kept at 70 °C for 4 h. Finally, the crude product was obtained after evaporating the solvent under reduce pressure. Dark yellow solid. It must be pointed out that it was difficult to purify the crude product to high purity, and although purification of PFBTPA was not attempted, we didn't regard it as a drawback for formation of SAMs because of the start material is not a surface-active chemical.^{40,41}

Synthesis of 4-perfluorohexyl-4'-(trichlorosilane)propoxyazobenzene (4b, PFHTPA)

The synthetic procedure was the same as that used for the synthesis of 4-perfluorobutyl-4'-(trichlorosilane)propoxyazobenzene (**4a**). Dark yellow solid.

Preparation of PFBTPA and PFHTPA SAMs on silicon substrates and isomerization of SAMs

The one-side polished silicon wafers were cut into several small rectangles (0.5×2 cm). These small rectangles were cleaned in acetone for 30 min by ultrasonic cleaner, and cleaned in ethanol for 10 min to remove organic impurities from the surfaces. Then, the cleaned silicon wafers were dried by N₂ gas. Subsequently, the silicon wafers underwent oxygen plasma processing (power = 100 W) for 10 min to obtain hydroxyl groups on the surface of silicon wafers. The hydroxylated silicon wafers were immediately put into a fresh solution of PFBTPA and PFHTPA about 1 % concentration (m/m, dissolved in toluene) for 30 min. Subsequently the silicon wafers were taken out of the solution, washed with toluene and dried in N₂ gas.^{35,40}

The isomerization of the SAMs was achieved by UV irradiation and heat treatment (Figure 9). In order to obtain a transformation from *trans* isomer to *cis* isomer, we have put the SAMs into a long wave-length UV device (BZZ200G-T, 200-W) using light of 40 mW/cm². Then, we heated the SAMs, which had been irradiated by UV light, to 160 °C to obtain back the *trans* isomer.

Acknowledgements

We gratefully acknowledge the financial support by the National Natural Science Foundation of China (No. 51273140), Jiangsu Overseas Research & Training Program for University Prominent Young & Middle-aged Teachers and Presidents, and the Project Funded by the Priority Academic Program Development of Jiangsu Higher Education Institutions.

References

1. Iqbal, D.; Samiullah, M.; *Materials (Basel)* **2013**, 6, 116–142.
2. Dincer, S.; Tamerler, C.; Sarikaya, M.; Piskin, E. *Surf. Sci.* **2008**, 602, 1757–1762.
3. Liu, Y.; Mu, L.; Liu, B.; Kong, J. *Chem. Eur. J.* **2005**, 11, 2622–2631.
4. Sun, T.; Feng, L.; Gao, X.; Jiang, L. *Acc. Chem. Res.* **2005**, 38, 644–652.
5. Nath, N.; Hyun, J.; Ma, H.; Chilkoti, A. *Surf. Sci.* **2004**, 570, 98–110.
6. Rzaev, Z. M. O.; Dinc, S.; Pis, E. *Prog. Polymer Sci.* **2007**, 32, 534–595.
7. Liu, R.; Xiao, Q.; Li, Y.; Chen, H.; Yan, Z.; Zhu, H. *Dyes Pigm.* **2011**, 92, 626–632.
8. Raposo, M. M. M.; Fonseca, A. M. C.; Castro, M. C. R.; Belsley, M.; Cardoso, M. F. S.; Carvalho, L. M.; Coelho, P. J. *Dyes Pigm.* **2011**, 91, 62–73.
9. Ning, Z.; Tian, H. *Chem. Commun.* **2009**, 37, 5483–5495.
10. Lim, H. S.; Han, J. T.; Kwak, D.; Jin, M.; Cho, K. *J. Am. Chem. Soc.* **2006**, 128, 14458–14459.
11. Siemeling, U.; Rittinghaus, S.; Weidner, T.; Brison, J.; Castner, D. *Appl. Surf. Sci.* **2010**, 256, 1832–1836.
12. Dalkiranis, G. G.; Therézio, E. M.; Da Silva, M. A. T.; Poças, L. C.; Duarte, J. L.; Laureto, E.; Dias, I. F. L.; Tozoni, J. R.; Silva, R. A.; Marletta, A. *J. Lumin.* **2013**, 134, 842–846.
13. Micheletto, R.; Yokokawa, M.; Schroeder, M.; Hobara, D.; Ding, Y.; Kakiuchi, T. *Appl. Surf. Sci.* **2004**, 228, 265–270.

14. Duan, J.; Wang, M.; Bian, H.; Zhou, Y.; Ma, J.; Liu, C.; Chen, D. *Mater. Chem. Phys.* **2014**, 148, 1013–1021.
15. Wolf, M.; Tegeder, P. *Surf. Sci.* **2009**, 603, 1506–1517.
16. Gan, S. M.; Pearl, Z. F.; Yuvaraj, A. F.; Lutfur, M. R.; Gurumurthy, H. *Spectrochim. Acta, Part A* **2015**, 149, 875–880.
17. Rau, H. *J. Photochem.* **1984**, 26, 221–225.
18. Feng, C. L.; Zhang, Y. J.; Jin, J.; Song, Y. L.; Xie, L. Y.; Qu, G. R.; Jiang, L.; Zhu, D. B. *Langmuir* **2001**, 17, 4593–4597.
19. Wang, G.; Song, Y.; Jiang, L. *J. Photochem. Photobiol., C* **2007**, 8, 18–29.
20. Rosario, R.; Gust, D.; Hayes, M.; Jahnke, F.; Springer, J.; Garcia, A. A. *Langmuir* **2002**, 18, 8062–8069.
21. Caputo, G.; Nobile, C.; Kipp, T.; Blasi, L.; Grillo, V.; Carlino, E.; Manna, L.; Cingolani, R.; Cozzoli, P. D.; Athanassiou, A. *J. Phys. Chem. C* **2008**, 112, 701–714.
22. Delorme, N.; Bardeau, J. F.; Bulou, A.; Poncin-Epaillard, F. *Langmuir* **2005**, 21, 12278–12282.
23. Brittain, W. J.; Siewierski, L. M.; Petrash, S.; Foster, M. D. *Polym. Prepr. (Am. Chem. Soc., Div. Polym. Chem.)* **1998**, 39, 264–265.
24. Jiang, W.; Wang, G.; He, Y.; Wang, X.; An, Y.; Song, Y.; Jiang, L. *Chem. Commun.* **2005**, 28, 3550–3552.

25. Jin, C.; Yan, R.; Huang, J. *J. Mater. Chem.* **2011**, 21, 17519–17525.
26. Wan, P.; Jiang, Y.; Wang, Y.; Wang, Z.; Zhang, X. *Chem. Commun.* **2008**, 44, 5710–5712.
27. Stevens, N.; Priest, C. I.; Sedev, R.; Ralston, J. *Langmuir* **2003**, 19, 3272–3275.
28. Cao, X. H.; Liu, X.; Chen, L. M.; Mao, Y. Y.; Lan, H. C.; Yi, T. *J. Colloid Interface Sci.* **2015**, 458, 187–193.
29. Lim, H. S.; Han, J. T.; Kwak, D.; Jin, M.; Cho, K. *J. Am. Chem. Soc.* **2006**, 128, 14458–14459.
30. Cai, L.; Li, Z. X. *Fibers Polym.* **2015**, 16, 2094–2105.
31. Liang, J. Y.; He, L.; Dong, X.; Zhou, T. *J. Colloid Interface Sci.* **2012**, 369, 435–441.
32. Cichomski, M.; Kosla, K.; Kozłowski, W.; Szmaja, W.; Balcerski, J.; Rogowski, J.; Grobelny, J. *J. Appl. Surf. Sci.* **2012**, 258, 9849–9855.
33. Cheng, D. F.; Masheder, B.; Urata, C.; Hozumi, A. *Langmuir* **2013**, 29, 11322–11329.
34. Acres, R. G.; Ellis, A. V.; Alvino, J.; Lenahan, C. E.; Khodakov, D. A.; Metha, G. F.; Andersson, G. G. *J. Phys. Chem. C* **2012**, 116, 6289–6297.
35. Wu, L.; Cai, L.; Liu, A.; Wang, W.; Yuan, Y.; Li, Z. *Appl. Surf. Sci.* **2015**, 349, 683–694.
36. Zhou, X. Y.; Wang, G.; Lei, T. *Phosphorus, Sulfur Silicon Relat. Elem.* **2013**, 188, 701–710.
37. Miao, X. R.; Cheng, Z. Y.; Ren, B. Y.; Deng, W. L. *Surf. Sci.* **2012**, 606, L59–L63.
38. Paik, M. Y.; Krishnan, S.; You, F.; Li, X.; Hexemer, A.; Ando, Y.; Kang, S. H.; Fischer, D. A.; Kramer, J. E.; Ober, Ch. K. *Langmuir* **2007**, 23, 5110–5119.

39. Lei, H.; Liu, J.; Song, L.; Shen, Y.; Haughey, S. A.; Guo, H.; Yang, J.; Xu, Zh.; Jiang, Y.; Sun, Y. *Molecules*. **2011**, 16, 7043–7057.
40. Siewierski, L. M.; Brittain, W. J.; Petrash, S.; Foster, M. D. *Langmuir* **1996**, 12, 5838–5844.
41. Haensch, C.; Hoepfner, S.; Schubert, U. *Spec. Publ. - R. Soc. Chem.* **2010**, 39, 2323–2334.
42. Szwajca, A.; Wei, J.; Schukfeh, M. I.; Tornow, M. *Surf. Sci.* **2015**, 633, 53–59.
43. Sato, T.; Tsuji, K.; Kokuryu, E.; Wadayama, T.; Hatta, A. *Mol. Cryst. Liq. Cryst.* **2003**, 1, 13–39.
44. Natansohn, A.; Rochon, P. *Chem. Rev.* **2002**, 102, 4139–4175.
45. Gautam, S.; Balijepalli, S.; Rutledge, G. C. *Macromolecules* **2000**, 33, 9136–9145.
46. Akiyama, H.; Tamada, K.; Nagasawa, J.; Abe, K.; Tamaki, T. *J. Phys. Chem. B* **2003**, 107, 130–135.
47. Zhang, X.; Wen, Y.; Li, Y.; Li, G.; Du, S.; Guo, H.; Yang, L.; Jiang, L.; Gao, H.; Song, Y. *J. Phys. Chem. C* **2008**, 112, 8288–8293.
48. Cai, Y.; Liu, M.; Hui, L. *Ind. Eng. Chem. Res.* **2014**, 53, 3509–3527.

Table 1 Chemical composition of PFBTPA SAMs before and after heat treatment

Peak	Position (eV)	Mass concentration (%)	
		Before heat treatment	After heat treatment
C	282.5	46.13	43.76
O	529.3	13.26	12.27
Si	99.2	8.49	8.35
N	391.1	3.85	4.38
F	687.1	28.26	31.24

Table 2 Surface roughness of the silicon substrate and PFBTPA assembled on the silicon

Samples	Ra (nm)	Rq (nm)
Silicon substrate	0.255	0.322
PFBTPA SAMs	0.591	0.826

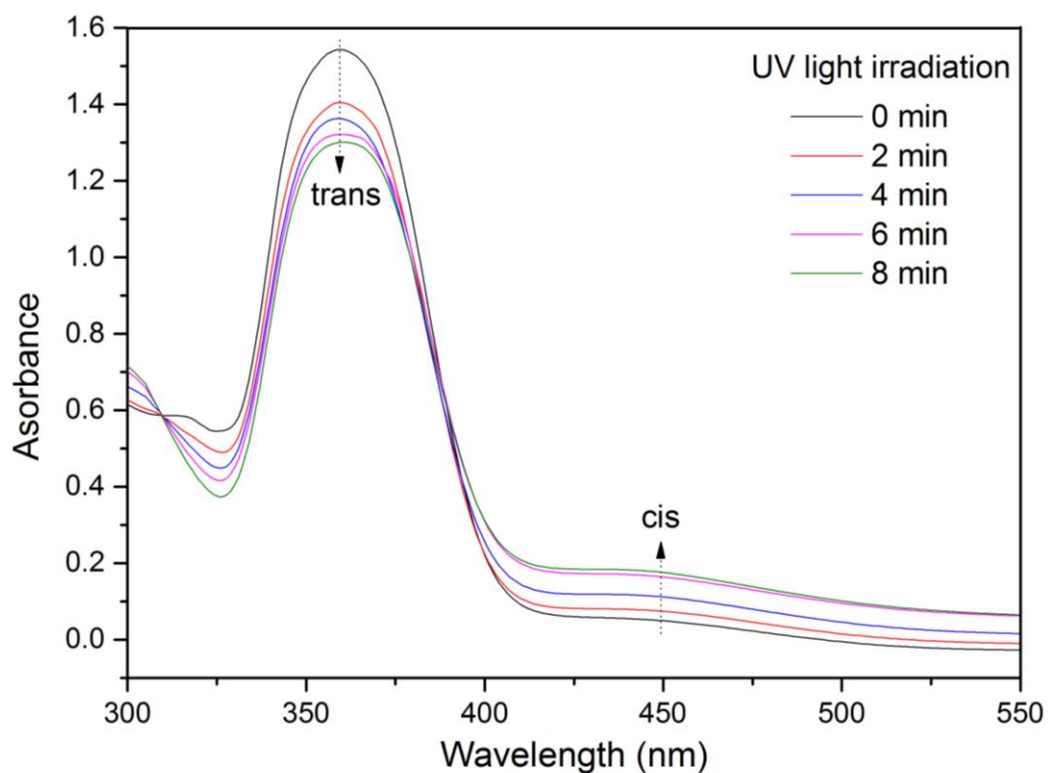


Figure 1 UV-visible absorption spectra of PFBTPA monomers dissolved in toluene solution and irradiated with UV light for different time periods

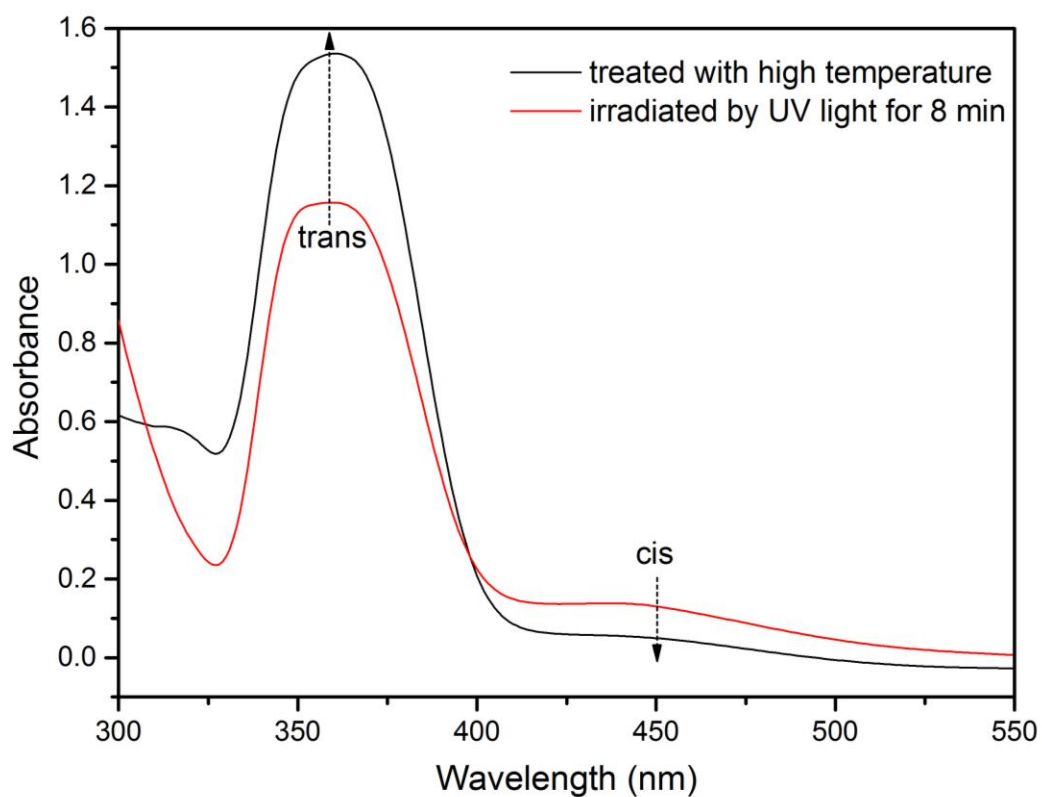


Figure 2 UV-visible absorption spectra of PFBTPA monomers dissolved in toluene solution (which had been irradiated by UV light for 8 min) and after being heated to 80 °C for 1h

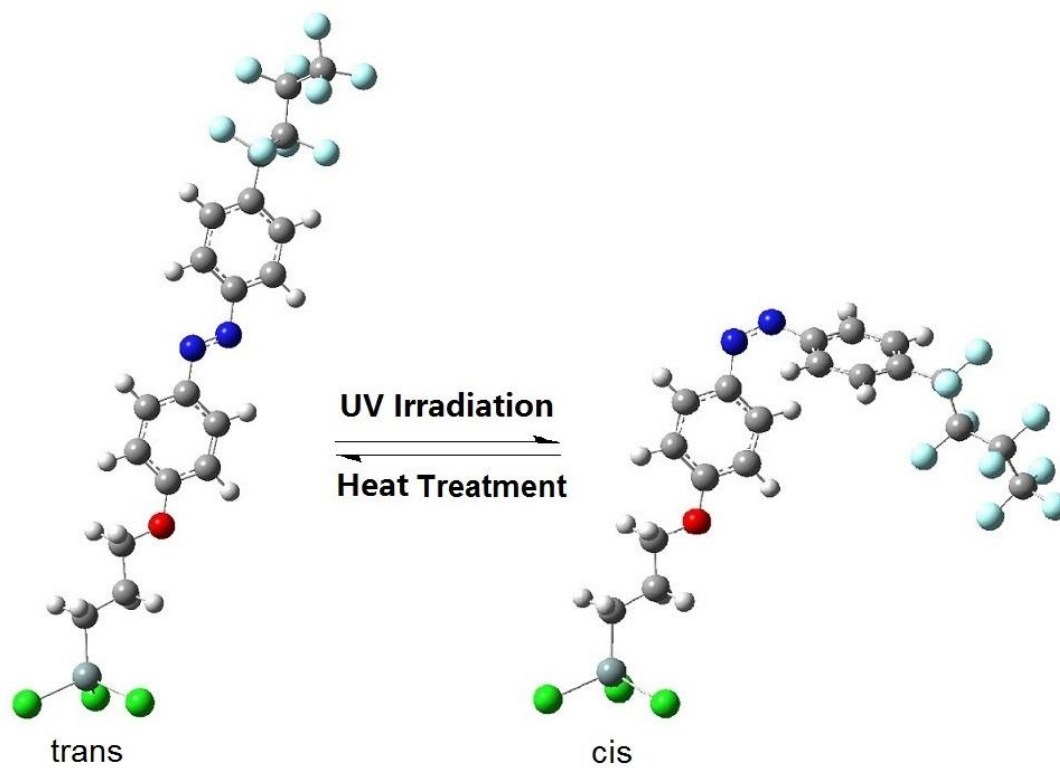


Figure 3 Change in conformation during the optothermal isomerization of PFBTPA

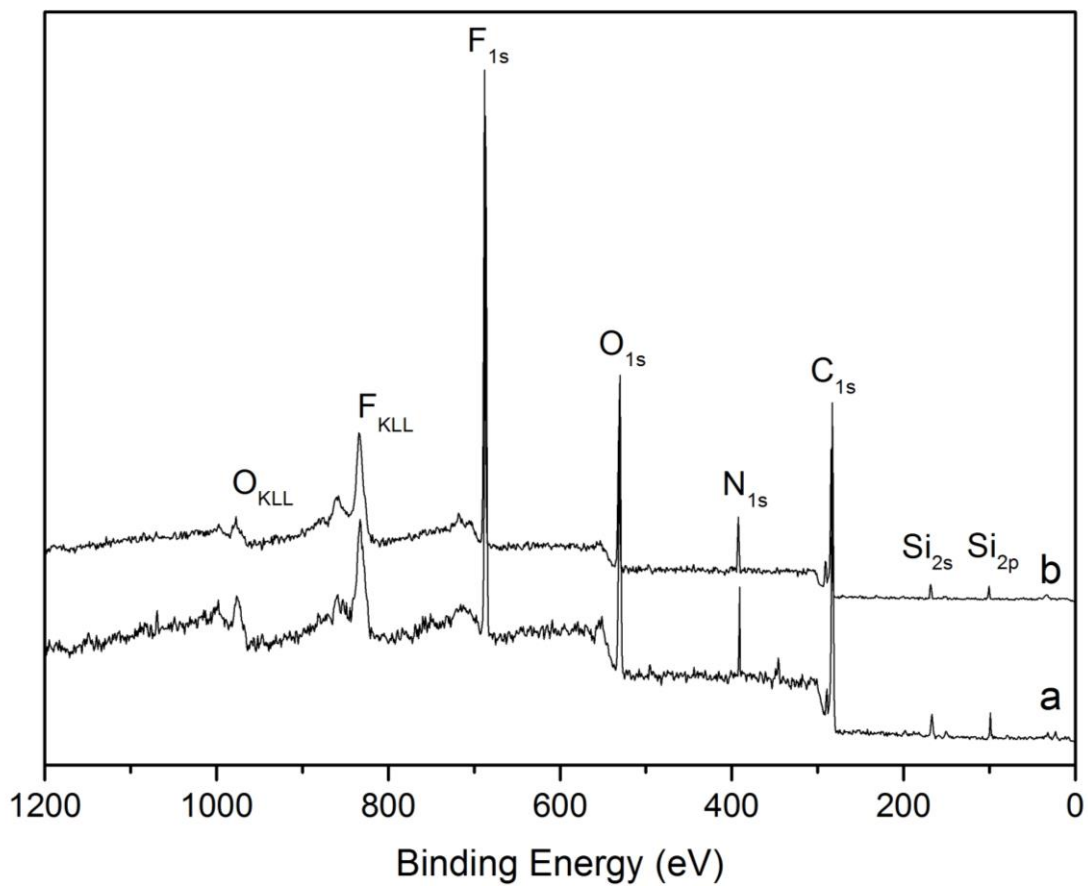
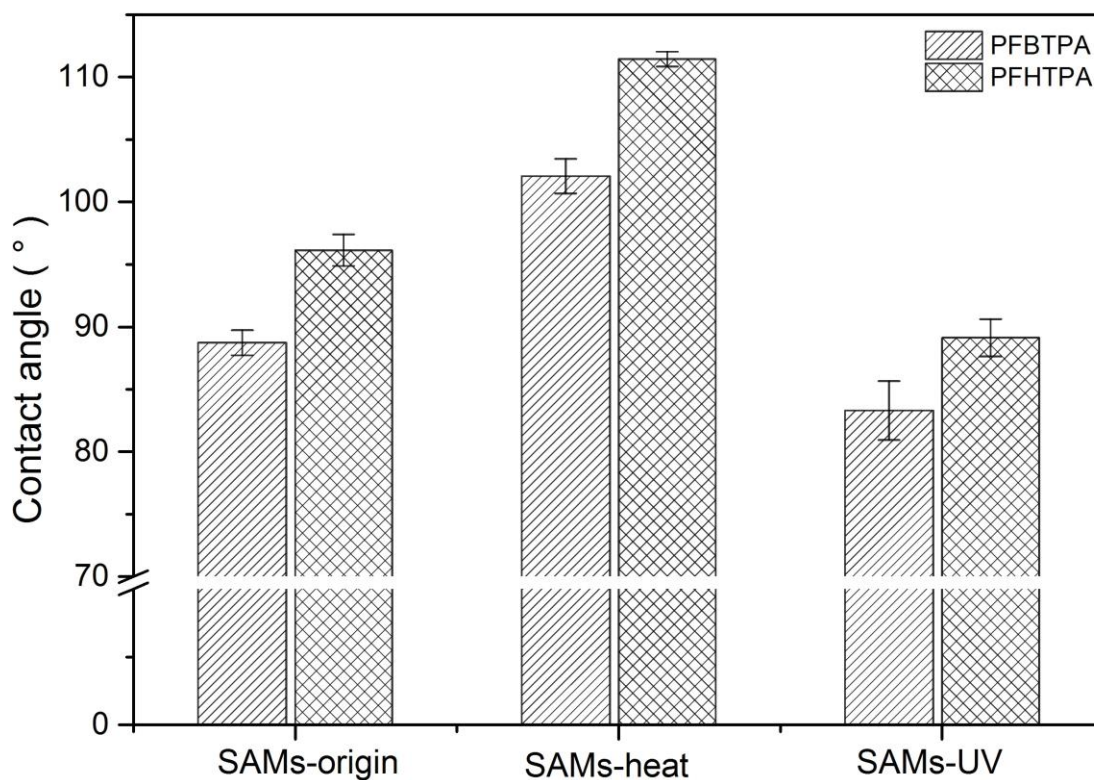


Figure 4 XPS of PFBTPA SAMS before (a) and after (b) heat treatment



SAMs-origin: without any treatment; SAMs-heat: treated with high temperature;

SAMs-UV: irradiated by UV light for 10 minutes

Figure 5 The contact angles of PFBTPA SAMs and PFHTPA SAMs undergoing different treatment

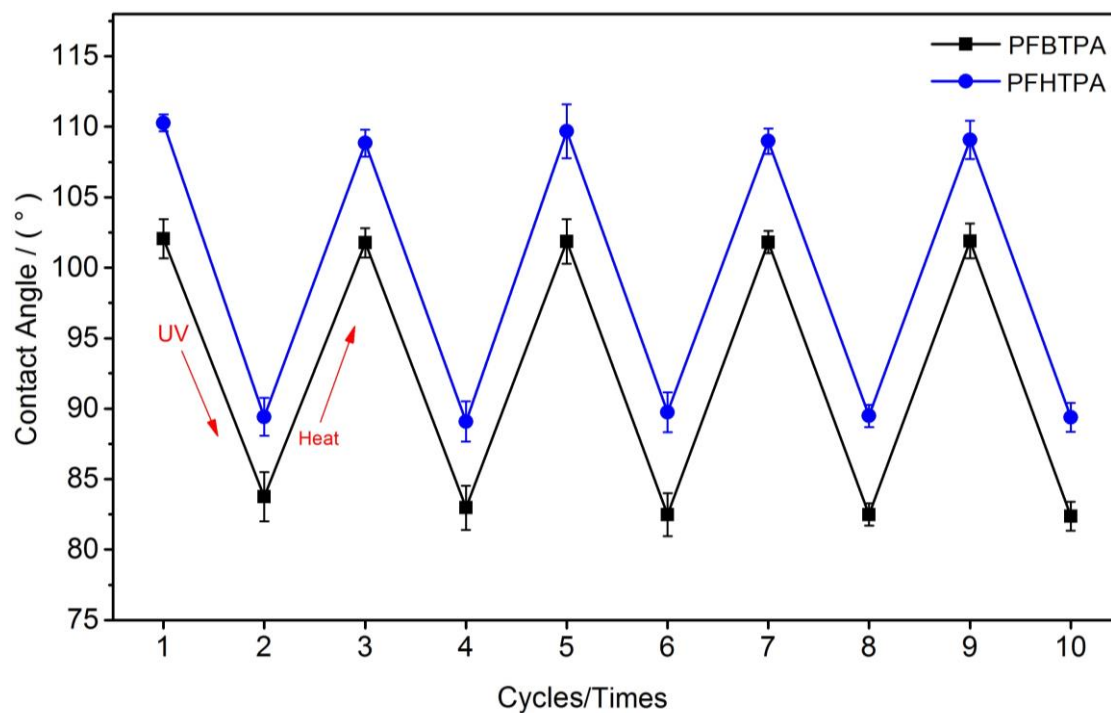


Figure 6 Reversible wettability of PFBTPA SAMs and PFHTPA SAMs on silicon substrates (UV: the SAMs on silicon substrate were irradiated by long-wave UV light for 10 min; Heat: the irradiated SAMs on silicon substrate were heated to 160 °C in bake oven)

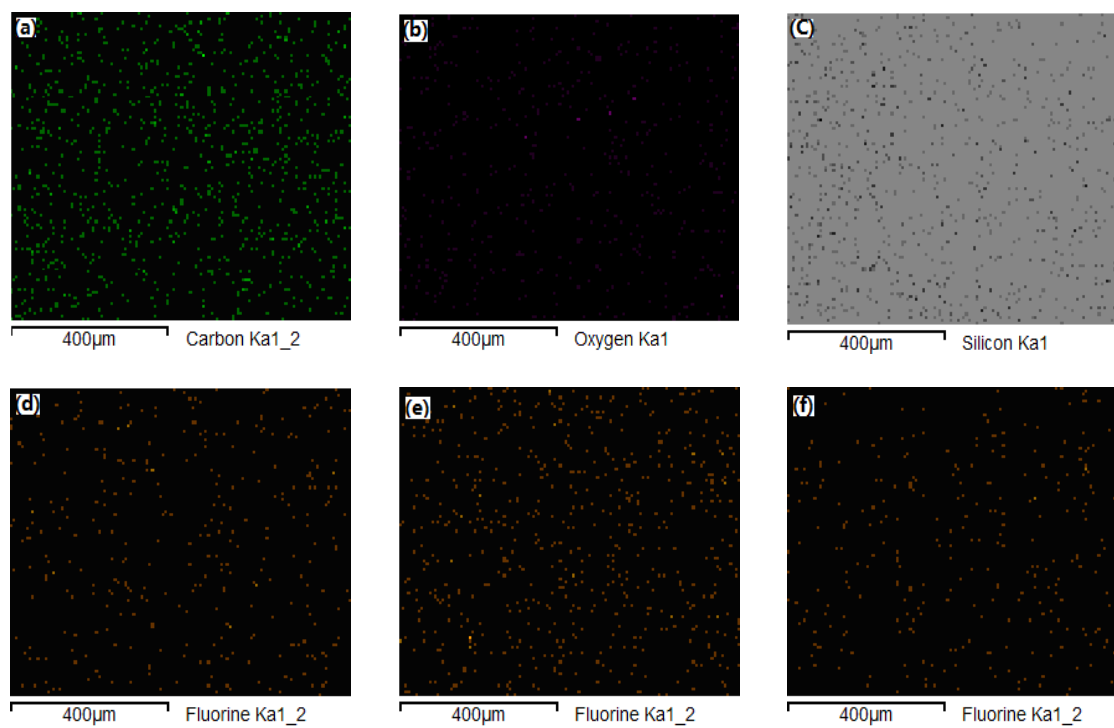


Figure 7 Element composition of PFBTPA SAMs after different treatments: without any treatment (a-C, b-O, c-Si, d-F); heated to 160 °C for 1 h (e-F); irradiated by UV light for 10 min (f-F)

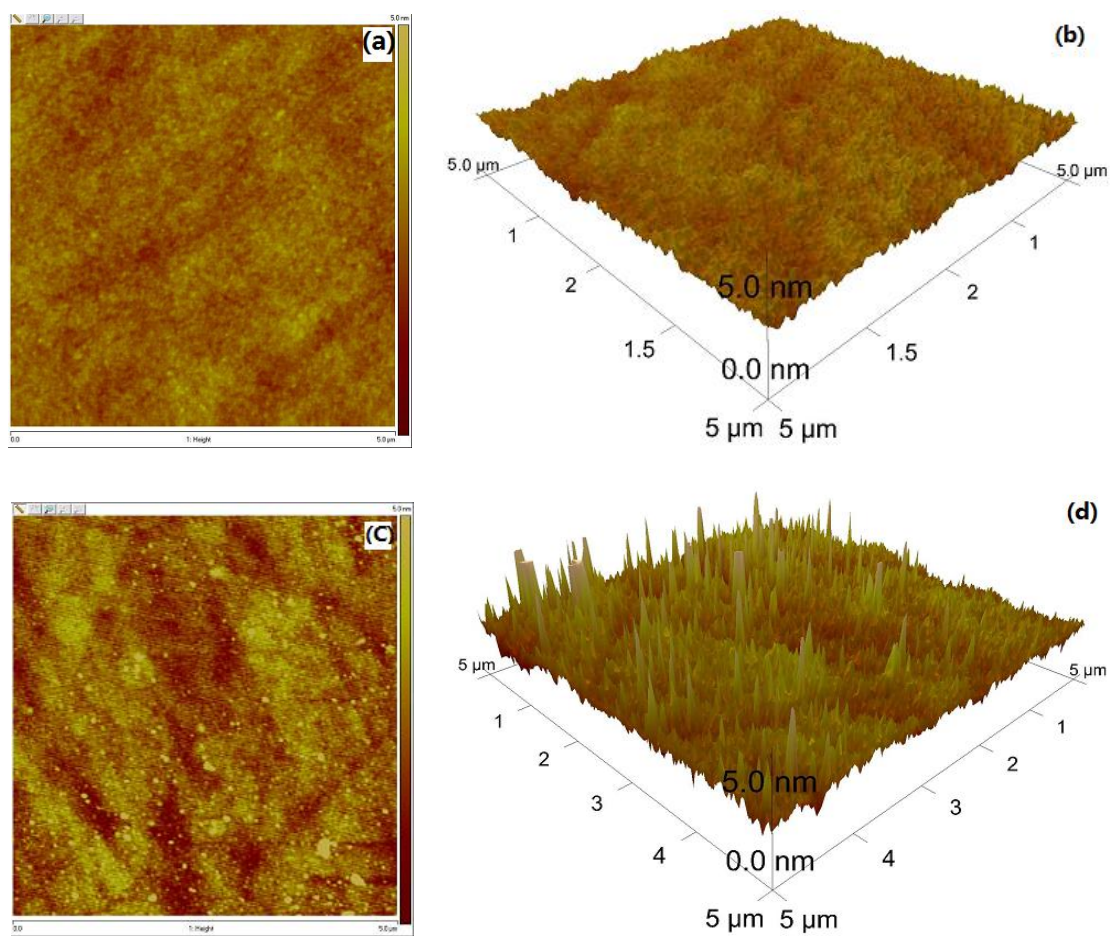


Figure 8 2D and 3D AFM images of bare silicon substrate (a-2D, b-3D), and PFBTPA SAMs (c-2D, d-3D)

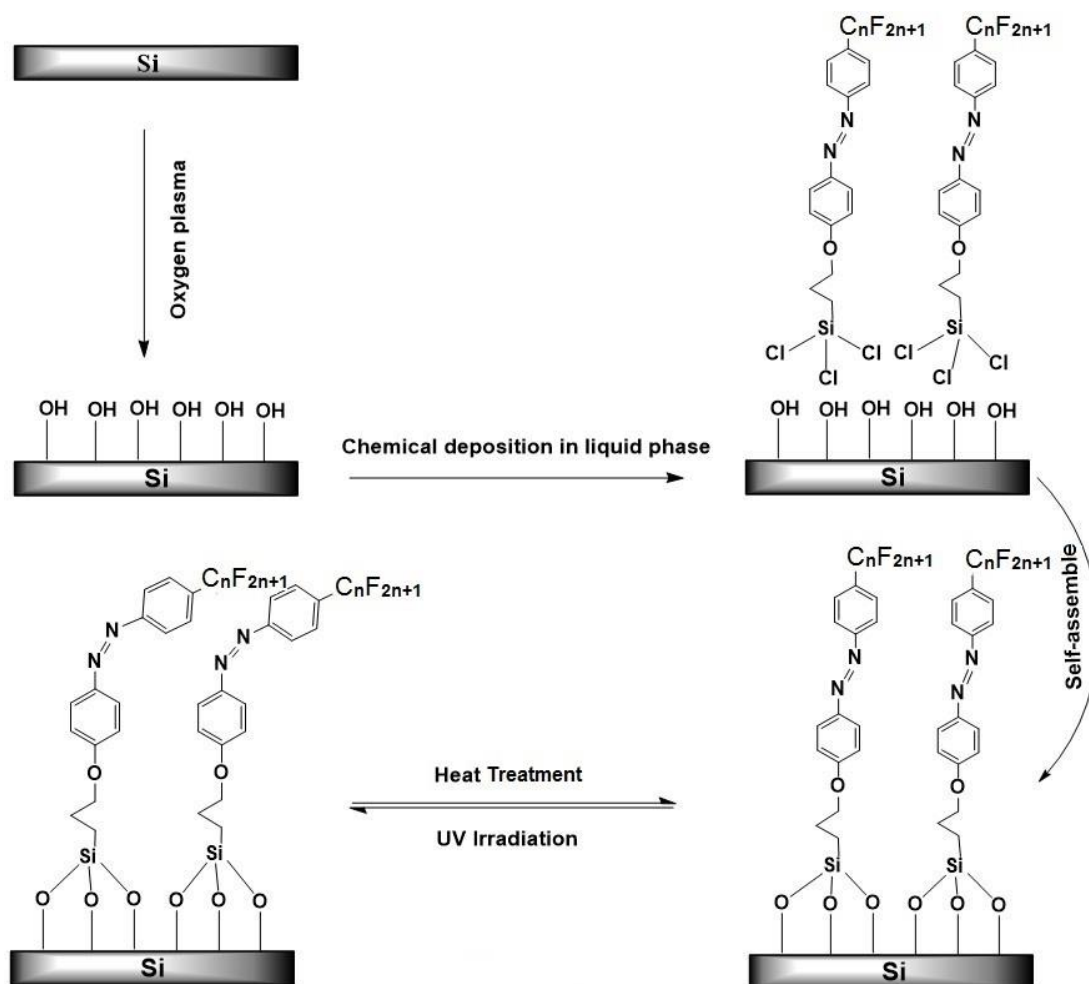
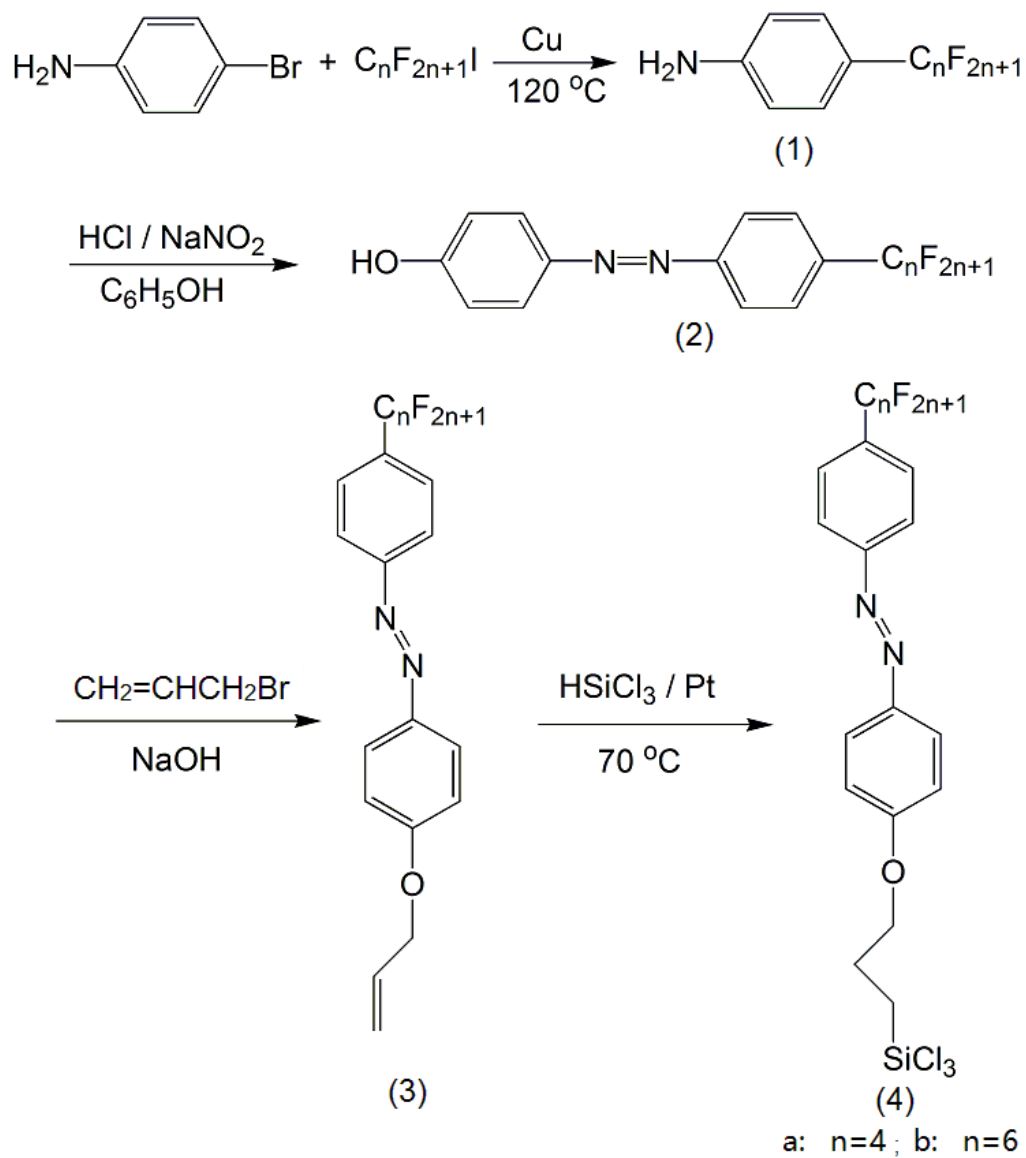


Figure 9 Preparation of SAMs on silicon substrates and isomerization of SAMs ($n = 4$ or 6)



Scheme 1 Synthesis of the perfluoroalkyl azobenzene trichlorosilane monomers